Structural study of the smectic-*I* to smectic-*F* transition in freely suspended films

J. A. Collett and P. T. Kondratko
Department of Physics, Lawrence University, Appleton, Wisconsin 54912

M. E. Neubert
Liquid Crystal Institute, Kent State University, Kent, Ohio 44240

(Received 22 December 1999; revised manuscript received 28 July 2000)

The smectic-*I* (S_I) to smectic-*F* (S_F) phase transition in terephthal-bis-(4*n*)-decylaniline (TB10A) has been examined for a possible continuous transition via the intermediate smectic-*L* (S_L) phase. X-ray diffraction measurements of thick, single-domain, freely suspended films are used to classify the phases and to determine the hexatic order parameter C_6 and its harmonics. Instead of the continuous transition suggested in the literature we find a first-order $S_I \rightarrow S_F$ transition with a discontinuous change in the direction of the bond-orientational order relative to the molecular tilt. The tilt of the molecular form factor in the hexatic phases is inconsistent with the tilt estimated from published layer spacing measurements, suggesting that the hexatic phases of TB10A must have the molecular cores oriented at an angle relative to the tails. This result taken together with published results on the S_C phase suggests that the $S_C \rightarrow S_I \rightarrow S_F$ transitions are driven by changes in the conformation of the hydrocarbon tails. Examination of the harmonic scaling relation between the hexatic order parameters shows mean-field behavior in the S_I phase. This result will make binary mixtures of TB10A with other materials a practical system for the study of the crossover from mean field to the *XY* behavior seen in other hexatic systems.

PACS number(s): 64.70.Md, 61.10.Eq, 61.30.Eb, 68.35.Rh

I. INTRODUCTION

Defect-mediated models of phase transitions have generated considerable interest in condensed matter physics. Halperin and Nelson's theory of a continuous, defect-mediated, melting transition [1] predicts that two-dimensional triangular solids will melt into two-dimensional liquids via a two-step process. In the first step, pairs of bound dislocations (vacancies) unbind to leave a fluid that retains bond-angle orientation. In the second step, the free dislocations dissociate into free pairs of disclinations which destroy the bond-angle orientational order. The intermediate phase is called hexatic in recognition of the sixfold rotational symmetry of the phase. The two-step melting sequence provides a framework for classification of smectic liquid crystal phases with the hexatic smectic-*B* phases and the smectic-*I* (S_I), smectic-*F* (S_F), and smectic-*L* (S_L) phases modeled as stacks of two-dimensional hexatic layers.

Although the liquid crystal phase sequence mirrors the defect-mediated melting theory, the details of the transitions do not. Without exception, the transition from the hexatic phase to the crystalline phase in liquid crystals is discontinuous. The transition from hexatic to fluid may be continuous, but its critical exponents do not fall into the expected three-dimensional (3D) *XY* model universality class [2]. Since the hexatic-to-fluid transition is not quantitatively described by the simple disclination unbinding model, there must be another mechanism involved in the transition. This mechanism may involve interaction of bond-orientational order with molecular tilt, or changes in the conformation of the individual molecules that change the energetics of disclination binding. The several hexatic liquid crystal phases provide a rich system for the study of hexatic order.

Liquid crystal systems exhibit a number of tilted hexatic phases with at least quasi-long-range order in bond orientation and molecular tilt, but short-range crystalline order. Figure 1 shows how the S_I, S_F, and S_L phases are differentiated by the angle between the local bond-angle direction and the azimuthal projection of the molecular tilt. The S_I and S_F phases have the projection of the molecular tilt into the layer plane making angles with the local bonds of 0° and 30°, respectively, while the S_L phase has a projection that makes an azimuthal angle ϕ between 0° and 30° with respect to local bond directions [3]. The S_I and S_F phases can transform into the S_C phase via the loss of bond-orientation order. The S_I and S_F phases have been identified in a number of thermotropic liquid crystals with a limited number of those compounds exhibiting both phases [4,5]. Lyotropic systems have exhibited the S_L phase [9] in which the azimuthal angle varies between 0° and 30°. Optical observations of stripe-

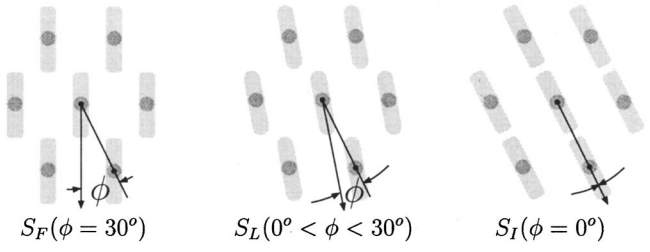

FIG. 1. The different projections of the director onto the plane of the layers in the S_F, S_I, and S_L phases are shown. The angle ϕ is the angle between the hexatic reference direction and the projection of the director onto the plane of the layers. The S_F phase has the projection of the director lying midway between adjacent molecules ($\phi = 30°$), the S_I phase has the projection lying directly along a line connecting two neighboring molecules ($\phi = 0°$), and the S_L phase covers all intermediate orientations.

defect domains in freely suspended thin films of FTE1 suggest that surface S_L phases exist [6]. Electron diffraction measurements in films show coexistence of S_L surface phases up to 11 layers thick on top of S_C interior layers [7,8]. There has still been no conformation of the S_L phase in bulk thermotropic liquid crystals. Terephthal-bis-(4n)-decylaniline (TB10A) has been reported to have S_C, S_I, and S_F phases [4,10] with the $S_C \rightarrow S_I$ transition reported as first order and the $S_I \rightarrow S_F$ transition reported as possibly continuous [11,13]. If the transition is truly continuous, it should occur via the intermediate S_L phase and would provide the first example of the bulk S_L phase in a thermotropic liquid crystal.

The theory of tilted hexatic phases was presented by Nelson and Halperin [14] and extended by Selinger and Nelson (SN) [15] to include transitions between the different tilted phases by the addition of terms in the Hamiltonian describing the interaction between the local bond-orientation field $\theta(\mathbf{r})$ and the local tilt-azimuthal angle field $\phi(\mathbf{r})$. The interaction term in the mean-field Landau-Ginzburg Hamiltonian is expressed as

$$V(\theta-\phi) = -h_6 \cos[6(\theta-\phi)] - h_{12} \cos[12(\theta-\phi)]. \tag{1}$$

If $h_{12} \geqslant 0$, a first-order $S_I \rightarrow S_F$ transition is predicted as h_6 goes from positive to negative. If $h_{12} < 0$, the system could evolve continuously from $S_I \rightarrow S_L \rightarrow S_F$ with ϕ increasing continuously from 0° to 30° as the temperature decreases and h_6 goes from positive to negative. The theory also predicts a continuous $S_I \rightarrow S_F$ transition when the tilt elastic constants are below critical values. Since the elastic constants are expected to scale with the number of layers in the sample, a continuous transition directly from S_I to S_F is not expected in bulk samples.

The $S_I \rightarrow S_F$ transition has been noted in several compounds but carefully examined in only a few. The dynamics of the weakly first order $S_I^* \rightarrow S_F^*$ transition in 4-(2′-methylbutyl) phenyl 4-(*n*-octyl) biphenyl-4-carboxylate has been studied by light scattering in a five layer freely suspended film [16] and by dielectric spectroscopy in bulk samples [17]. The details of the $S_I^* \rightarrow S_F^*$ transition were not reported in the earlier x-ray investigation of this material [18]. The S_I and S_F phases have also been found in x-ray scattering studies of thin films of 4-*n*-heptyloxybenzylidene-4-*n*-heptylaniline, but the $S_I \rightarrow S_F$ transition was not examined [19–21]. Studies of FTE1 [6–8] show a continuous transition in a surface phase in a system which has no hexatic phases in bulk. This paper presents a detailed x-ray study of the hexatic order and its relation to the molecular tilt at the $S_I \rightarrow S_F$ transition in a bulk thermotropic system. We find a first-order transition with coexisting S_I and S_F phases and no S_L phase.

In addition to examining the $S_I \rightarrow S_F$ transition, we also studied the nature of the bond orientation order in the S_I phase of TB10A. Bond-orientational order in TB10A is of interest since mixtures of TB10A with 4-n-decyloxy biphenyl 4-(2′-methylbutyl) benzoate show a $S_C \rightarrow S_I$ critical point where the transition changes from first order to continuous [22]. Measurements of the harmonic scaling in the hexatic order parameters should reflect the nearby first-order transition and set the stage for studies of orientational order in mixtures near the critical point. The transition to hexatic bond-orientational order is thought to be in the 3D *XY* universality class unless it is affected by the presence of nearby tricritical point [23]. Hexatic ordering has been measured in TB5A, TB6A, and TB7A [24], homologues of TB10A, to investigate the effect of increasing the temperature difference between the fluid-to-hexatic transition ($S_C \rightarrow S_F$) and the hexatic-to-crystal transition ($S_F \rightarrow S_G$). They speculate that the presence of a hexatic to crystal transition below the fluid to hexatic transition is the reason that mean field behavior is seen in harmonic scaling near the $S_C \rightarrow S_I$ transition. Since the temperature difference between the $S_C \rightarrow S_I$ and the $S_F \rightarrow S_G$ transitions in TB10A is nearly 40 °C, the impact of crystalline ordering on the $S_C \rightarrow S_I$ transition should be minimized. Instead we have the much weaker hexatic to hexatic transition below the S_I phase. Harmonic scaling analysis [23–26] has been used to determine the role of order parameter fluctuations in the S_I phase of TB10A. We find mean-field behavior in the S_I phase rather than the *XY* behavior seen in TB7A, suggesting that the bond orientation fluctuations are being suppressed by the first-order $S_C \rightarrow S_I$ transition rather than by a nearby hexatic to crystal transition.

Measurements of the azimuthal projection of the molecular tilt and the hexatic order parameters are obtained by analysis of x-ray scattering data from single-domain, freely suspended films of TB10A. We use a magnetic field to orient the molecular tilt and exploit the weak coupling between the molecular tilt and bond-orientational order to produce large, oriented, hexatic domains that can be studied in the vicinity of the transition. We use an area detector to map out large regions of reciprocal space. From these maps, we determine positional correlation lengths, the hexatic order parameters, and the direction of the molecular tilt. The hexatic order parameters are extracted by Fourier analysis of the scattering data, and the molecular tilt direction is inferred from the effect of the molecular form factor on the two-dimensional structure factor that describes the hexatic phase. The mapping of large regions of reciprocal space assures us that we are sensitive to any shifts in domain makeup and also to scattering that may develop in nearby regions.

The rest of this paper is organized as follows. Section II describes measurement and analysis techniques. Section III presents the x-ray scattering data used to determine the structures of the S_I and S_F phases. Separate subsections discuss structure related to molecular tilt and hexatic bond angle orientation. Section IV contains a discussion of the results and a comparison of our measurements with published measurements on hexatic phases of TB10A and other compounds. Based on our structural determination together with other published measurements on S_C phase of TB10A, we propose a model of the $S_C \rightarrow S_I \rightarrow S_F$ transitions in TB10A based on conformational changes in the hydrocarbon tails. Results of harmonic scaling analysis show that bond orientation fluctuations in the S_I phase of TB10A behave according to mean field theory. Section V contains a brief summary of important results. Appendix A contains a detailed description of the local lattices and structure factors of the S_I, S_F, and S_L phases.

II. EXPERIMENTAL METHODS

Thick films of TB10A [27] are produced by using a stainless steel wiper to spread the liquid crystal in the S_C phase across a 7 mm hole in a thin stainless steel plate. These films are allowed to equilibrate until the film is uniform and stable. The films are milky white in reflected white light and have thickness greater than 1.5 microns (500 layers) [21]. The oven is equipped with 0.75 inch diameter $SmCo_5$ permanent magnets with a 0.75 inch gap that are used to provide a magnetic field of about 1.8 kG; the magnetic field, oriented in the plane of the liquid crystal film, aligns the director in the S_C phase before cooling to the hexatic phases. Temperature is controlled to 20 mK with differences of less than 4 mK across the illuminated volume of the film.

X-ray scattering measurements are made on a Bruker AXS GADDS (General Area Diffraction System) using the 10 cm×10 cm Hi-Star detector. The Hi-Star detector is a multiwire proportional counter with a spatial resolution of about 0.2 mm in each direction. The details of the resolution function will be published elsewhere [28,29]. The measured longitudinal resolution of the instrument is 0.031 $Å^{-1}$ full width at half maximum (FWHM) while the FWHM in the two transverse directions are 0.03 and 0.01 $Å^{-1}$. The resolution is well matched to the in-plane width of the hexatic peaks, which range from 0.01 to 0.04 $Å^{-1}$ in the S_I and S_F phases of TB10A.

At each temperature, we combine data from 124 exposures (frames) of the detector taken at different sample orientations into a single data array used to map the structure factor of TB10A. Once the large array is created, we display the structure in three dimensions, plot isosurfaces, extract data in planes with arbitrary orientation, and plot data along desired lines in reciprocal space.

The analysis of the x-ray scattering data is based upon the Birgeneau-Litster model of the S_I and S_F phases as stacks of weakly coupled two-dimensional hexatic layers [30]. The structure factor in the plane of the layers (the xy plane) is determined by the structure within the individual layers while the strength of the scattering out of the plane of the layers is determined purely by the molecular form factor. The weak coupling between layers produces uniform bond orientation and makes the bond order truly long range. The structure factor in the plane of the layers for an ideal two-dimensional hexatic phase will have six fuzzy columns perpendicular to the xy plane; the cross section of the columns can be described by a Lorentzian function with a FWHM of $2/\xi$, where ξ is the correlation length for crystalline order within the two-dimensional layer. The strength of the scattering in the z direction is determined by the molecular form factor of the molecules that make up the hexatic layer. Since the molecules are approximated to first order by elongated cylinders, contours of constant form factor will look similar to flattened ellipsoids with the major axes perpendicular to the long axis of the liquid crystal molecule. The result of the product is a set of six fuzzy spots located in the reciprocal space plane that includes the origin and is oriented perpendicular to the long axes of the molecules.

We model the in-plane structure as a distorted triangular lattice. In the absence of molecular tilt, the primitive triangular lattice is spanned by equal length vectors with an angle of 60° between them. The presence of the molecular tilt breaks the sixfold symmetry, causing a distortion in the lattice along the direction of the projected tilt. If we assume that the molecular tilt preserves the area of the unit cell in the plane containing the director and the normal to the smectic layers (the tilt plane), the resulting lattice can be described in terms of a lattice constant a, a packing tilt β_p, and an azimuthal angle ϕ describing the orientation of the director relative to the underlying bond directions. The appendix presents the derivation of the reciprocal lattice vectors associated with tilted hexatic phases.

Molecular tilt has proven difficult to determine in tilted smectic phases [11,12]. X-ray scattering experiments usually estimate molecular tilt by measuring the smectic layer spacing and determining the tilt angle that yields a projection of the extended molecular length on to the layer normal that equals the layer spacing. Our experiment determines the tilt of the molecular core by measuring the distortion of the local two-dimensional hexatic lattice and by measuring the molecular form factor. We describe the local lattice distortion by the factor $1/\cos(\beta_p)$, the factor by which tilted cylinders must move apart when tilted toward one another if they are to preserve the density in the tilt plane. The angle β_p represents the tilt as measured by the packing distortion. Another measure of the molecular tilt angle and its orientation relative to the underlying hexatic order can be found by measuring the points where the disk with the maximum form factor intensity intersects the six columns of the hexatic structure factor. This angle is referred to as β_f, the molecular form factor tilt, since it is not necessarily the same as the angle β_p, which describes the distortion in the packing within the smectic layers. If both effects are dominated by the molecular core, we expect these two angles to be equal. We rely on published data for layer spacing as we cannot measure the layer spacing in our experimental configuration.

The azimuthal orientation of the tilt is most easily determined by finding the orientation of the molecular form factor. Figure 2 shows a plot of the out of plane (q_z) component of the scattering vector where the disk containing the major axes of the molecular form factor intersects the columns of the hexatic structure factor for the (10), (11), and (01) peaks. The peak locations in the figure were calculated by finding the intersection of vertical lines through each of the six peaks of the two-dimensional, psuedohexagonal structure with a plane through the origin normal to the director specified by the tilt angle $\beta_f=\beta_p=28°$, lattice constant $a=5.22$ Å, and azimuthal angle ϕ. See the Appendix for the details of the calculation. These plots are shown as a function of ϕ, which corresponds to $\phi-\theta$ in the theory of Selinger and Nelson. The S_I and S_F structures correspond to ϕ values of 0° and ±30°, respectively. Note that for any azimuthal orientation other than 0°, ±30° and equivalent angles, each of the six hexatic peaks assumes a different value of q_z. By finding the q_z value for each peak and by finding the plane which includes all six peaks, we can determine both β_f and ϕ. The widest peaks have a FWHM of $\Delta q_z=0.25$ $Å^{-1}$. The peak position can be located to about 10% of that value. For peaks near $q_z=0$, $|dq_z/d\phi|\approx 0.01$ $Å^{-1}$/deg. By measuring the difference in q_z between the peaks that are closest to $q_z=0$, ϕ is determined within ±2.5°.

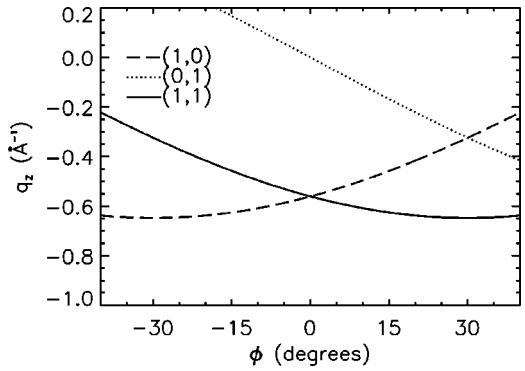

FIG. 2. This graph depicts the q_z position along a Bragg rod where the molecular form factor is maximized. The peak locations are plotted for three reciprocal lattice vectors as a function of ϕ, the angle between the projection of the director into the smectic layer plane and the direction of the local hexatic order. In the S_I phase ($\phi=0°$), the (10) and (11) peaks appear at equal, negative values of q_z, the (01) and $(0\bar{1})$ are at $q_z=0$, and the $(\bar{1}\bar{1})$ and $(\bar{1}0)$ peaks appear at equal, positive values of q_z. In the S_F phase ($\phi=30°$), the (11) and $(\bar{1}\bar{1})$ peaks are at opposite negative and positive values of q_z, the (10) and (01) peaks are at negative values of q_z that are exactly half that of the (11) peak, and the others are the reflections of these three. In the S_L phase all peaks occur at different values of q_z.

III. EXPERIMENTAL RESULTS

A. $S_I \rightarrow S_F$ structural transition

Reciprocal space maps were assembled at temperatures ranging from 130 to 154 °C with the most data collected near the $S_I \rightarrow S_F$ transition. This paper contrasts the S_F structure found at 151 °C with the S_I structure at 153 °C. The samples are oriented so that the xy plane is the plane of the smectic layers and the z axis is normal to the layers. When interpreting the reciprocal space maps, recall that the plane of strongest scattering is perpendicular to the long axis of the molecular core and that the six orientational ordering peaks in reciprocal space are related to the real space positions by a 30° rotation about the z axis if the packing is not distorted. We begin by reviewing the three-dimensional reciprocal space map and its projection onto the xy plane to discern the overall structure of the phase and the quality of the sample. We then extract a two-dimensional slice through the hexatic peaks along with linear plots through the peaks that are radial in the plane of the layers (q_r plots) and perpendicular to the layers (q_z plots). From these plots we determine the phase and the molecular tilt.

Figure 3 contrasts the structural maps in the S_F phase at 151 °C with the S_I phase at 153 °C. Figures 3(a) and 3(b) show three-dimensional threshold plots of all points with intensity greater than 20% of the maximum intensity. In both cases the molecular tilt is uniform across the illuminated portion of the sample since the hexatic peaks lie in a common plane. Figures 3(c) and 3(d) show the same data projected onto the xy plane. The arrows in the figure show the projection of the molecular tilt into the plane of the layers. Note that the tilt direction stays nearly the same in the two phases while the hexatic peaks rotate by 30° because the magnetic field is fixing the director of the molecules. The two short arcs of Figs. 3(a) and 3(c) are the ends of a single arc. Obstacles in the scattering setup prevented data collection in this region.

Figures 3(e) and 3(f) show planes that pass through the maxima of the peaks in Figs. 3(a) and 3(b), respectively. These planes represent the maximum of the molecular form factor and are perpendicular to the long axis of the molecules. From the orientations of these planes we can extract the molecular tilt β_f and the azimuthal projection angle ϕ. In the S_F phase Fig. 3(e) shows that the molecular cores are tilted by 28.3° from the smectic layer normal and make an angle of 59° with respect to the q_x axis of Fig. 3(c) when the tilt is projected into the smectic layer plane. Note that the peaks of Fig. 3(e) are close to lying on a circle while those of Fig. 3(c) do not. This shows that the tilting process is approximately volume conserving and that there is still a sixfold symmetry in the plane normal to the molecules. Any distortion from hexagonal symmetry in Fig. 3(e) indicates some loss of rotational symmetry, which suggests that molecules no longer freely rotate about their long axes. In the S_I phase at 153 °C, Fig. 3(f) shows that the molecules are tilted by 27.3° from the normal to the layers and that the azimuthal projection of the molecular tilt makes an angle of 56.5° with the q_x axis of Fig. 3(d). The peaks shown in Fig. 3(f) clearly lie on a circle, showing that the sixfold packing symmetry exists in the plane normal to the molecules. Note that the arcs in the S_F phase [Fig. 3(e)] are wider and less symmetric than the ones in the S_I phase [Fig. 3(f)]. This suggests either that the hexatic order parameter is not saturated, that there is a mosaic spread, or that the domain orientation shifted during the data collection period.

Table I summarizes the peak locations found by extracting q_z plots through the peaks shown in Figs. 3(g) and 3(h) and radial plots in the xy plane. Using Eqs. (A7), (A11), and these peak locations we can infer the tilt of the molecular form factor (β_f), the packing tilt (β_p), and the lattice constant. Fitting the radial plots using a power of a Lorentzian for the structure factor convolved with the instrumental resolution gives us the correlation lengths in each phase.

At 153 °C the peak locations in q_z along with the finite correlation length in the plane of the layers clearly demonstrate that the system is in the S_I phase. The adjacent peaks at $q_z=-0.55$ and -0.57 Å^{-1} flanked by peaks at $q_z=+0.01$ and -0.01 Å^{-1} are a clear signature of the S_I structure. Because the q_z peaks are not exactly at zero the scattering is also consistent with a S_L structure with an azimuthal orientation angle of $\phi=1.0\pm2.5°$. However, since we do not observe an increase in this angle as temperature is changed and since we observe coexistence with the S_F structure at 152 °C, we identify this as a S_I phase.

Figure 4 shows a radial plot in the xy plane through the peak at $q_z=0.01$ Å^{-1} at $T=153$ °C. The dashed line in the plot represents the instrumental resolution while the solid line represents the fit to the data. A correlation length of 114 Å was obtained for this peak by fitting the data to a convolution of a fractional power of a Lorentzian structure factor with the Gaussian instrumental resolution function. We use the fractional power to crudely take into account the resolution volume and variation in domain orientation. For a single domain sample and perfect resolution, one expects a Lorentzian shape, whereas a square root of a Lorentzian is expected in the case of a powder distribution in the plane of the layers

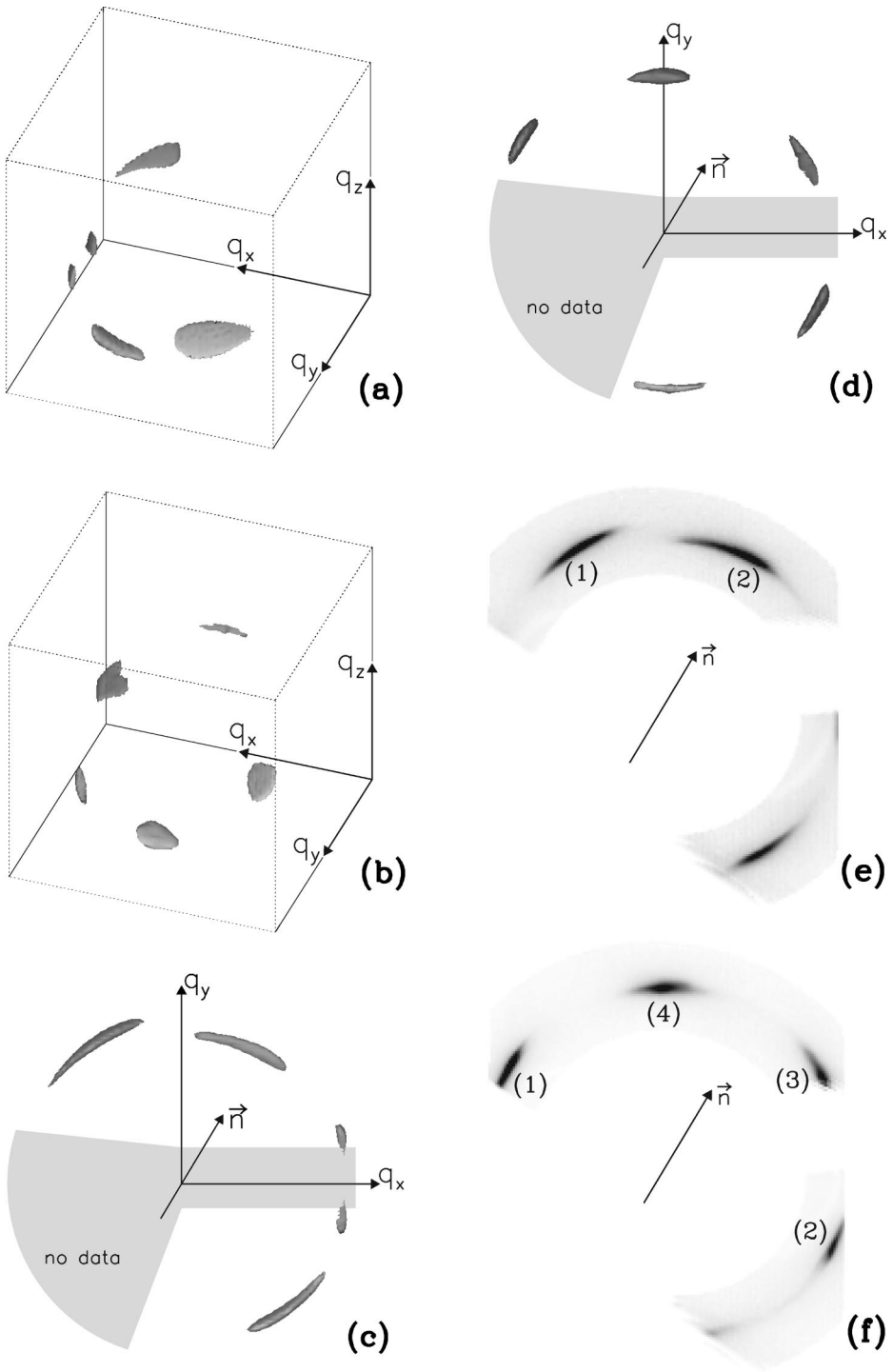

FIG. 3. Reciprocal space maps and slices in the S_F phase [(a),(c),(e),(g)] and S_I phase [(b),(d),(f),(h)] of TB10A at $T=151\,^{\circ}\mathrm{C}$ and $T=153\,^{\circ}\mathrm{C}$, respectively. (a),(b) These three-dimensional reciprocal space threshold plots show oblique views of all measured points in reciprocal space with intensity greater than 20% of the maximum intensity observed. (c),(d) These are the same data as in (a),(b) except that the map is viewed down the z axis (normal to the smectic layer planes). The inferred projection of the director onto the plane of layers is shown. The distortion of the in-plane packing from the molecular tilt causes the peak position along this direction to have a smaller component in the xy plane. (e),(f) Here we show an intensity plot in the plane where the molecular form factor is maximized. (g),(h) Plots of intensity vs q_z through peaks indicated in (e) and (f), respectively.

[25]. We find that the 0.9 power Lorentzian form fits these data better than a square root or a pure Lorentzian. This indicates that there is a small variation in the hexatic order direction across the beam. The radial correlation length for the peak at $q_z=-0.55\,\text{Å}^{-1}$ (at a 30° angle to the projection of the tilt into the xy plane) is 48 ± 10 Å, while the radial correlation length through the peak at $q_z=0.01\,\text{Å}^{-1}$ (perpendicular to the molecular tilt) is 114 ± 20 Å. We find that the correlation length along the projected direction of the molecular tilt is shorter than it is in the direction perpendicular to the tilt. This is consistent with previous reports on tilted hexatic phases [24,25]. The width of these peaks is in excess of the instrumental resolution, clearly showing that the crystalline order has limited range in the S_I phase.

At 151 °C the q_z locations of the peaks point to the S_F structure. The peak with the extreme value of q_z is flanked by two peaks with q_z positions half that of the extreme peak. Calculations of the molecular form factor tilt using Eq. (A11) give $\beta_f=28.8\pm0.7°$. This is consistent with the value 28.3° found by manually searching for the plane containing the peaks of the scattering. Fits of radial plots give correlation lengths of 60 Å in the direction of the molecular tilt projection into the layer plane [peak (2) in Fig. 3(e)] and 170 Å when the radial plot is directed through peak (1) of Fig. 3(e). In the S_F phase the structure factor is assumed to be a 0.6 power of a Lorentzian. The longer arcs in Fig. 3(c) indi-

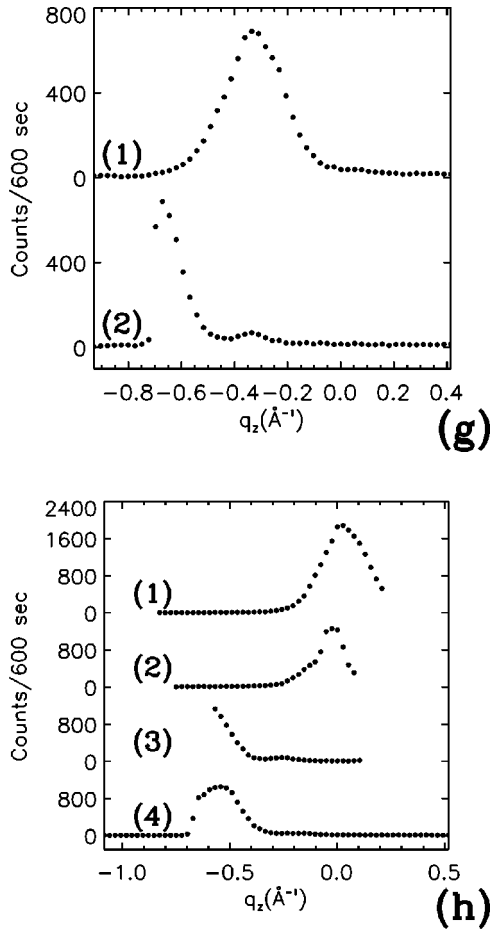

FIG. 3. (*Continued*).

cate a possibly larger mosaic spread consistent the lower power fit. As is expected, the correlation lengths in the lower temperature phase are longer than in the higher temperature S_I phase.

Given the uncertainties attributed to the form factor and packing tilts, a model in which the form factor tilt equals the packing tilt is consistent with measurements in both the phases. Table I shows the lattice constants and packing tilts β_p calculated from the positions of the peaks in the q_r plots using Eq. (A7). The packing tilt uncertainty in the S_I phase is larger than the corresponding uncertainty in the S_F phase because the position of the (11) S_I peak is less sensitive to molecular tilt than is the location of the (11) S_F peak.

Although molecular tilts measured by packing distortion and rotation of the molecular form factor are consistent with

TABLE I. Summary of peak positions, correlation lengths, and molecular tilts determined by the form factor and packing in the S_I phase and the S_F phase.

	S_I ($T=153°$)	S_F ($T=151°$)
q_z peaks (± 0.02 Å^{-1})	$-0.55, -0.57, \pm 0.01$	$-0.68, -0.33$
q_r peaks (± 0.01 Å^{-1})	1.40,1.28	1.36,1.24
Correlation length (Å)	48 ± 10, 114 ± 20	60 ± 20, 170 ± 30
Form factor tilt (β_f)	$27.9\pm 1.2°$	$27.5\pm 0.9°$
Packing tilt (β_p)	$27.7\pm 0.8°$	$28.8\pm 0.7°$
In-plane lattice constant	5.18 ± 0.04 Å	5.19 ± 0.04 Å

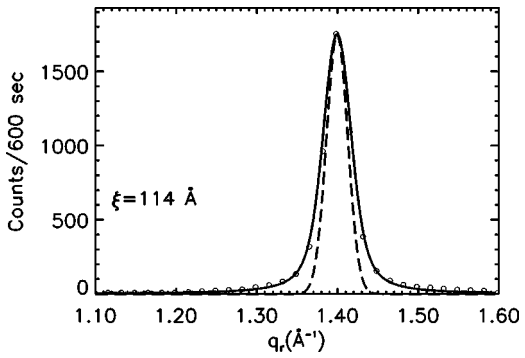

FIG. 4. Radial plot in the xy plane through peak (1) of Fig. 3(h) at $q_z=0.01$ Å^{-1}. Instrumental resolution is shown by a dashed curve on the plot. The solid line is a fit to the data using the convolution of a 0.9 power of Lorentzian structure factor with a Gaussian resolution function. The peak is located at $q_r=1.40$ Å^{-1} and has a width corresponding to a correlation length of 114 Å when fit using the 0.9 power Lorentzian. The peak is clearly wider than the instrumental resolution, proving that this is a true hexatic phase.

one another, they are not consistent with tilts of 22.7° to 26.8° obtained from previously published measurements of the smectic layer spacing [11,22]. The inconsistency between form factor and layer spacing measurements of molecular tilt suggests that the S_I and S_F phases may have molecules with the Z configuration first proposed by Bartolino *et al.* [12], in which the molecular cores have an orientation different from the hydrocarbon tails.

Coexisting S_I and S_F phases observed at 152 °C provide compelling evidence for a first-order hexatic to hexatic transition in TB10A. Multiple domains appear with q_z plots showing peaks at both the S_I and S_F positions. Preliminary data indicate that the form factor tilts are different for these two coexisting structures. When S_I and S_F phases coexist, the S_F phase forms with correlation lengths similar to the S_I phase although the fits are not as clean because of the coexisting peaks. The transition between S_I and S_F shows hysteresis with the transition observed at 152° while heating and at 150° upon cooling. The 2 °C range is probably caused by impurities or slow kinetics. There is no evidence of any intermediate S_L structure.

B. Hexatic order parameters

In addition to identifying the tilt orientation, we also measured the hexatic order parameters in the S_I phase of TB10A at 153 °C. Figure 3(f) shows data in the reciprocal space plane perpendicular to the director. Even though the structure in the plane of the layers does not have sixfold symmetry, the structure factor in the plane perpendicular to the director has sixfold symmetry about the director axis normal if the distortion caused by the tilt is volume conserving. Because of obstacles in the oven we cannot effectively fit the full circle but instead choose a single 60° segment around peak (d) in Fig. 3(f) for analysis. We extract 128 points from a 60° segment of the circle and perform a fast Fourier transform on the data to produce the structure factor

$$S(\chi)=\sum_{n=-64}^{64} A_n \exp(i6n\chi), \tag{2}$$

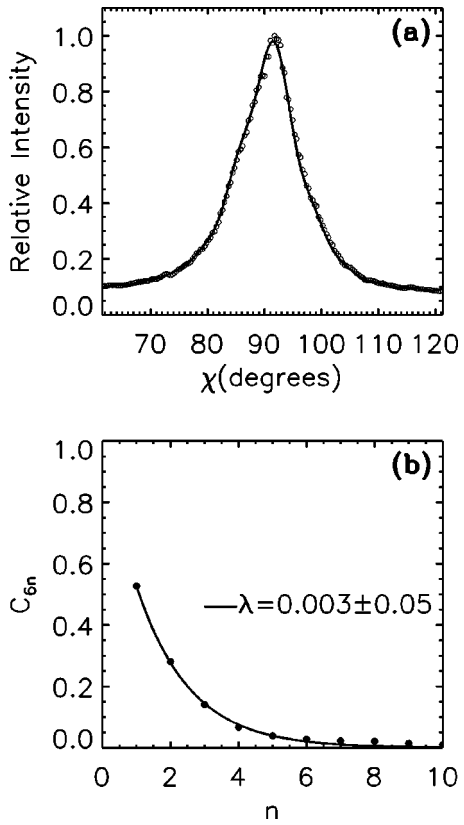

FIG. 5. (a) shows the 60° segment used to determine the harmonics of the hexatic order parameter. The solid line represents the fit obtained from the first ten terms in the expansion. (b) shows a plot of C_{6n} vs n for $n=1$ to 10. The solid line shows the best fit to Eq. (4), which produces a value of $\lambda=0.003\pm0.05$. The fit is consistent with $\lambda=0$, showing that the hexatic order parameter fluctuations at 153 °C are described by mean-field theory.

where the coefficients A_n are the complex Fourier coefficients. This expression maps to the form used by Noh *et al.* [24],

$$S(\chi)=I_0\left[\frac{1}{2}+\sum_{n=1}^{\infty} C_{6n}\cos\{6n(\chi-\chi_0)\}\right], \qquad (3)$$

if we identify $I_0=2A_0$ and $C_{6n}=|A_n|/A_0$. The peak position χ_0 is contained in the phases of the complex Fourier coefficients but is not calculated since it is not relevant to the orientational order parameter. We do not include a background term in the fit because we have explicitly subtracted a measured background prior to the analysis. The constants C_{6n} are the order parameters of bond orientational order. The normalization of the order parameters is chosen so that all $C_{6n}\to 1$ as the orientational order assumes the form of a Dirac delta function.

We choose a χ peak with no nearby obstacles for fitting. Figure 5(a) shows the segment chosen and the fit obtained from the first ten terms in the expansion. Figure 5(b) shows a plot of the hexatic order parameters C_{6n} vs n along with a fit to the theoretical form

$$C_{6n}=C_6^{n+\lambda(T)n(n-1)}, \qquad (4)$$

TABLE II. Summary of all tilt determinations. The published layer spacings are from the literature. The layer spacing tilts in the last row are calculated from the published layer spacings.

	S_I ($T=153°$)	S_F ($T=151°$)
Packing tilt (β_p)	$27.9\pm1.2°$	$27.5\pm0.9°$
Form factor tilt (β_f)	$27.7\pm0.8°$	$28.8\pm0.7°$
Published layer spacing	38.0 Å,[a] 37.2 Å[b]	
Layer spacing tilt (β_l)	22.7°, 26.8°	

[a]Reference [11]. These measurements showed no change at the $S_I\to S_F$ transition.
[b]Reference [22]. This measurement was made in the S_I phase just below the $S_C\to S_I$ transition.

suggested by harmonic scaling theory when the order parameter becomes large [23]. At $T=153\,°$C, this fit produces $\lambda=0.003\pm0.05$, consistent with a zero value. The small value of λ shows that fluctuations in the hexatic order parameter are not important and that a mean field description of hexatic order is adequate for TB10A in the vicinity of the first-order transitions to the S_C phase at higher temperatures and the S_F phase at lower temperatures.

IV. DISCUSSION

A. $S_I\to S_F$ transition

In TB10A the transition from the S_I to S_F is clearly first order. The coexistence of both phases at 152 °C together with absence of any peaks that can be clearly identified as S_L preclude the existence of the S_L phase in bulk TB10A. Neither the tilt of the molecular form factor nor the correlation length in the plane of the layers changes dramatically at this transition. As we heat the sample out of the S_F phase, the tilt of the molecular form factor decreases by about 1° as the sample enters the S_I phase. Within the framework of the SN theory, a first-order transition means that $h_{12}>0$ and h_6 is changing from negative to positive as the temperature increases. Preliminary data indicate the form factor tilts of the S_I and S_F phases differ when they coexist, suggesting a change in the molecular conformation at the transition that could give rise to the change in h_6.

Table II summarizes our molecular tilt measurements along with published layer spacing measurements [11,22] and the molecular tilts inferred from these layer spacings using a rigid rod model of the molecule. The form factor and packing tilts are consistent with one another within each phase. Comparison of the form factor tilt measurements with published smectic layer spacing measurements shows that it is unlikely that the molecules in either phase can be modeled as fully extended, linear structures. If we assume that the molecules are rigid rods of length 41.7 Å [31] and that the tilt of the molecular form factor represents the tilt of the rigid rod, we would predict a smectic layer spacing of $(41.7\,\text{Å})\cos(27.7°)=36.9\,$Å in the S_I phase. This is below the reported values of 37.2 Å [11] and 38.5 Å [22] from the literature. In the S_F phase this model predicts a layer spacing of $(41.7\,\text{Å})\cos(28.8°)=36.5$ Å, a significant discrepancy with the published value and directly in opposition to the published claim of a layer spacing that increases as the temperature decreases. The last row of Table II gives the rigid

molecule tilts that would be required to match the two published layer spacings. The measured form factor and packing tilts exceed these values although the extreme low end of the S_I range comes close to the tilt one calculates if the layer spacing is assumed to be 37.2 Å.

If the layer spacing in the films is the same as reported in bulk TB10A, the resolution of the layer spacing conflict may lie in conformation of the tails of the molecule. The *Z* conformation of Bartolino [12] in which the hydrocarbon tails are parallel to each other but at an angle to the rigid core provides one plausible explanation. The chemical structure of terephthal-bis-(4*n*)-decylaniline is given by

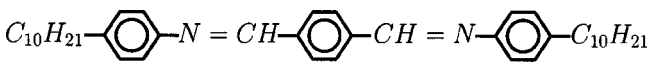

The core of the molecule contains three phenyl groups and is a rigid, all trans, structure of length 17.1 Å while the decyl chains at either end of the molecule have a length of just over 12 Å when fully extended. The decyl chains may have a slightly shorter effective length in these phases because of the presence of gauche conformations [11], although packing considerations constrain the chains to nearly linear conformations. The electron density is highest in the rigid core region so this part of the molecule will make the largest contribution to the form factor. If we assume that the cores are tilted by 28° relative to the layer normal and that the end chains are tilted by 18° to 26° relative to the layer normal, we recover layer spacings of 38.5 to 37.2 Å, consistent with published results. That is, the average direction of the tails would have to differ by 2° to 10° from the core's orientation. The difference could be greater if the tails went off in a different azimuthal direction. For this explanation to work, the directions of the end chains must be strongly correlated with one another. This means that there must be some loss of rotational freedom in the hexatic phases. The form factor should contain one part reflecting the core tilt and another weaker piece reflecting the end chains. If the orientations of the chains are strongly correlated, the molecular form factor should be asymmetric in q_z with a longer tail on the low q_z side of the peak. This is what we see in our q_z plots.

We propose that the transition from the fluid S_C phase to the hexatic S_I phase is driven by a conformational change from linear structure to the *Z* structure. When layer spacing measurements in the S_C phase [11,22] are examined the tilt angle is predicted to be between 26° and 30°, consistent with the form factor tilt that we measure in the S_I phase. The tails adopt the *Z* configuration while the cores maintain essentially the same relationship to each other. Bartolino [12] had observed that molecules in the S_C phase of TBBA, a shorter homologue of TB10A, behave nearly as rigid rods. It is plausible that the longer homologues also behave in this way in their S_C phases although we have no form factor measurements to confirm this hypothesis. The transition from fluid to hexatic results from a change to the *Z* configuration, thereby changing the energy associated with disclination defects. An alternative interpretation would have the *Z* configuration present even in the S_C phase with the transition to the hexatic phases driven by a chain freezing transition. This is also possible since measurements in the S_A phase [11] show a layer spacing about 2 Å less than the fully extended molecular length.

The transition from $S_I \rightarrow S_F$ probably involves a further conformational change that changes the interaction between the molecular tilt and the hexatic bond angle orientational order parameters. Preliminary data show that the form factor tilt in the S_I phase is greater than the tilt in the S_F phase when they coexist at 152 °C. The end chain tilt could change or reorient relative to the core to maintain the layer spacing. This hypothesis cannot be confirmed without more detailed quantitative analysis of the molecular form factors and the generation of specific structural models. Single-domain hexatic films provide the setting in which such models might be rigorously tested.

B. Harmonic scaling

Finally, we address the issue of bond orientational order in the S_I phase of TB10A. The higher order hexatic order parameters are fit to the form

$$C_{6n} = C_6^{\sigma_n},$$

$$\sigma_n = n + \lambda n(n-1), \tag{5}$$

in the region where the hexatic order is well developed as a way of probing the nature of the fluctuations present in the hexatic system. This approach applied to 8OSI gives $\lambda = 0.295$ when measured 1 to 5 °C below the transition temperature [23–26]. While this form is derived in the critical region, it is valid when the order parameter grows sufficiently large. In three dimensions, $\lambda = 0.3$ if fluctuations are of the *XY* model type and $\lambda = 0$ if fluctuations are unimportant (mean-field theory). Since the transition from $S_C \rightarrow S_I$ is first order we cannot use the fits to derive parameters of the Landau-Ginzburg Hamiltonian [24] used to calculate the relations (5) but we can still use Eq. (5) to determine the nature of the order present in the system. When we fit the hexatic order parameters from TB10A at 153° we find a value of λ consistent with zero. This result is exactly what is expected in the vicinity of a first-order transition, but differs somewhat from the results on the homologues TB5A, TB6A, and TB7A. A study of the hexatic order in these compounds [24] yielded the $\lambda = 0.08$, 0.00, and 0.30, respectively, with the largest value occurring in TB7A. We find evidence for nothing other than mean-field behavior in TB10A. We are unable to get reliable measures of the order parameters at higher temperatures because the domain structure seems unstable, possibly because of coexistence with the S_C phase. In addition, the relatively short positional correlation lengths may reduce the strength of the coupling between the tilt and bond orientational order. We were unable to model the hexatic order parameter in the S_F phase. Although sharp peaks in the orientational plots appear, there are at least two closely spaced domains in each sample which make it impossible to cleanly extract the higher order hexatic order parameters.

The S_I structure in TB10A is similar to what has been observed in other compounds [25,26]. We find the same asymmetry in the in-plane correlation lengths with the length being longest in the direction perpendicular to the tilt plane.

The hexatic order in the S_I phase of TB10A is weaker than the order observed deep in the S_I phase of 8OSI since the magnitude of C_6 is 0.6 compared with 0.9 in 8OSI. Our TB10A correlation lengths correspond to values obtained in 8OSI at about 76°, two degrees below the $S_C \rightarrow S_I$ transition. At this temperature the fitted value of λ for 8OSI was 0.295 and unchanging. Aharony *et al.*, [23] hypothesized that λ decreased toward zero as the $S_C \rightarrow S_I$ transition was approached because of the presence of a tricritical point in the hexatic phase diagram. We have measured hexatic order in a S_I system known to be near the first-order $S_C \rightarrow S_I$ transition and have verified that this system shows mean-field behavior. This creates the possibility of studying the crossover to XY behavior in mixtures. Future studies using mixtures of TB10A with another S_I phase with a continuous transition will attempt to directly observe crossover to XY behavior as the critical point is passed.

V. SUMMARY

This experiment was undertaken with three intentions; to examine a potentially continuous $S_I \rightarrow S_F$ transition for the existence of the intermediate S_L phase, to characterize the nature of the bond orientational order in a S_I phase below a known first order $S_C \rightarrow S_I$ transition, and to learn more about the differences between the two hexatic phases with identical symmetry groups. The study of nearly single-domain, freely suspended films using reciprocal space mapping has partially answered these questions and pointed out promising avenues for future study. In contrast with previous results, we find that the transition from S_I to S_F in TB10A is first order with no hint of the intermediate S_L phase. Unlike its shorter homologues, TB10A's critical orientational fluctuations do not play a significant role in the hexatic S_I phase that comes immediately below the S_C phase. Harmonic scaling analysis of the higher order hexatic order parameters gives λ consistent with zero, the value for a system described by mean-field theory. Studies of mixtures will press this study beyond the critical point where we expect to find crossover to XY behavior. Finally, we have noted that the tilt of the molecular form factor in the S_I and S_F phases is inconsistent with a structure made up of fully extended molecules. We suggest that the $S_C \rightarrow S_I \rightarrow S_F$ transitions are driven by conformational changes in the hydrocarbon tails which leave the rigid molecular cores unchanged. Quantitative models of the effects of changing molecular shapes on the molecular form factor together with additional measurements on single domain samples will test this hypothesis in the future.

ACKNOWLEDGMENTS

One of us (J.A.C.) gratefully acknowledges helpful conversations with Larry Sorensen. We also acknowledge the work of James Truitt and Michael Stenner in developing the reciprocal space mapping software and the work of Ed Jalosynski in producing the liquid crystal oven. Joshua Cross, assisted with the quantitative measurement of instrumental resolution. This work was financially supported by the Research Corporation, the Donors of the Petroleum Research Fund, Lawrence University, and by the Exxon Education Foundation. The TB10A material was synthesized by Larry Maurer of the Organic Synthesis and Purification Group at Kent State. We acknowledge support from the ALCOM/NCIPT Resource Facility supported by NSF Grant No. DMR89-20145 and DARPA Contract No. MDA972-90C-0037.

APPENDIX: TILTED HEXATIC STRUCTURES

The tilted hexatic phases can be described in terms of two-dimensional structures. Although the hexatic phases involve stacks of layers, scattering measurements show that the only correlation in order from layer to layer is in the direction of the tilt and in the direction of bond orientational order. We can then model the scattering by assuming a set of independent two-dimensional layers with their axes aligned with one another. When scattering from planar structures is analyzed, the three-dimensional structure factor is written as the product of the molecular form factor and the two-dimensional structure factor describing the in-plane distribution of molecules:

$$S_{3D}(q_x,q_y,q_z)=S_{2D}(q_x,q_y)f_m(q_x,q_y,q_z). \qquad \text{(A1)}$$

Because hexatic phases have in-plane correlation lengths of 50 to 250 Å, the molecules have local order that appears crystalline over distances of 10 to 50 times the molecular spacing. With order this well developed, it is useful to develop a direct lattice and a reciprocal lattice to describe the two-dimensional order. While we know that there is no true crystal, the reciprocal lattice vectors represent the major Fourier components of the electron density. In this appendix the two-dimensional reciprocal lattice associated with tilted hexatic phases is developed for an arbitrary tilt direction and applied to the S_I and S_F structures. The molecular form factor is then introduced to determine the expected locations of the scattering peaks in the direction perpendicular to the layers(z) for any given tilted hexatic structure.

Hexatic phases with molecular tilt (S_I, S_F, and S_L) are characterized by two angles; θ characterizes the orientation of the local triangular lattice and ϕ describes the projection of the director into the plane of the smectic layers. Because the system is symmetric with respect to a simultaneous, uniform rotation of both angles, only the difference between them is crucial to the structure. In this section we will define one of the lattice directions to be $\theta=0$, leaving us with ϕ to deal with. The S_I and S_F phases are characterized by $\phi=0°$ and $\phi=30°$, respectively, while the S_L phase has an intermediate tilt direction. In the absence of the molecular tilt, the in-plane structure is assumed to have sixfold rotational symmetry. The presence of the molecular tilt breaks that symmetry and introduces a distortion into the triangular lattice. In this appendix the structure factor for tilted hexatic phases is developed.

We begin the calculation by assuming a two-dimensional symmetric triangular lattice with lattice constant a. The x axis of the system is chosen to be along one of the triangular lattice vectors. Before tilt is considered the undistorted primitive lattice vectors

$$\mathbf{a_{1u}}=a(1,0), \qquad \text{(A2)}$$

$$\mathbf{a_{2u}} = a\left(\frac{1}{2}, \frac{\sqrt{3}}{2}\right) \tag{A3}$$

span the direct lattice. When molecules tilt by β_p toward the direction described by the azimuthal angle ϕ, the molecular spacing increases along the tilt direction by the factor of $1/\cos(\beta_p)$ and remains unchanged in the direction perpendicular to the tilt. This factor describes the volume conserving distortion that would tilt close packed, hard cylinders in a common direction while keeping the perpendicular distance between adjacent cylinder axes constant. This is an oversimplification of the liquid crystal molecules, but it does provide a reasonable description if we assume that the molecules rotate freely and independently of one another. To calculate the distortion we introduce unit vectors $\mathbf{n}_1 = (\cos\phi, \sin\phi)$ and $\mathbf{n_2} = (-\sin\phi, \cos\phi)$, oriented parallel to and perpendicular to the projection of the director into the layer plane. Write the undistorted lattice vectors as linear combinations of $\mathbf{n_1}$ and $\mathbf{n_2}$, apply the distortion to the $\mathbf{n_1}$ component, and return to the original x and y coordinates. The resulting vectors are given by

$$\begin{aligned}\mathbf{a}_1 &= \frac{1}{\cos\beta_p}(\mathbf{a_{1u}}\cdot\mathbf{n_1})n_1 + (\mathbf{a_{1u}}\cdot\mathbf{n_2})\mathbf{n_2} \\ &= a\left[\sin^2\phi + \frac{\cos^2\phi}{\cos\beta_p}, \cos\phi\sin\phi\left(\frac{1}{\cos\beta_p} - 1\right)\right]\end{aligned} \tag{A4}$$

and

$$\begin{aligned}\mathbf{a_2} &= \frac{1}{\cos\beta_p}(\mathbf{a_{2u}}\cdot\mathbf{n_1})\mathbf{n_1} + (\mathbf{a_{2u}}\cdot\mathbf{n_2})\mathbf{n_2} \\ &= a\left[\frac{\cos\phi\sin(\phi+\pi/6)}{\cos\beta_p} - \sin\phi\cos\left(\phi+\frac{\pi}{6}\right),\right. \\ &\quad \left.\frac{\sin\phi\sin(\phi+\pi/6)}{\cos\beta_p} + \cos\phi\cos\left(\phi+\frac{\pi}{6}\right)\right].\end{aligned} \tag{A5}$$

The primitive reciprocal lattice vectors $\mathbf{b_1}$ and $\mathbf{b_2}$ must satisfy the relations

$$\begin{aligned}&\mathbf{b_1}\cdot\mathbf{a_1} = 2\pi, \quad \mathbf{b_1}\cdot\mathbf{a_2} = 0, \\ &\mathbf{b_2}\cdot\mathbf{a_1} = 0, \quad \mathbf{b_2}\cdot\mathbf{a_2} = 2\pi,\end{aligned} \tag{A6}$$

and are found to be

$$\begin{aligned}\mathbf{b_1} &= \frac{4\pi\cos\beta_p}{\sqrt{3}a^2}(a_{2y}, -a_{2x}), \\ \mathbf{b_2} &= \frac{4\pi\cos\beta_p}{\sqrt{3}a^2}(-a_{1y}, a_{1x}).\end{aligned} \tag{A7}$$

The distortion in the lattice changes the area of the unit cell by a factor of $1/\cos\beta_p$, independent of the azimuthal tilt direction ϕ. These primitive vectors span the xy plane of reciprocal space for any value of ϕ and are appropriate for the S_L phase. The lattices for the S_I and S_F phases can be found by substituting $\phi = 0$ and $\phi = \pi/6$, respectively.

If we write general reciprocal lattice vectors in terms of their Miller indices as $\mathbf{G_{hk}} = h\mathbf{b_1} + k\mathbf{b_2}$, the only observed peaks in the hexatic phases are Lorentzian peaks at the $(hk) = (10)$, (11), (01), $(\bar{1}0)$, $(\bar{1}\bar{1})$, and $(0,\bar{1})$ positions. Because this is a two-dimensional structure, the structure factor $S_{2D}(\mathbf{G_{hk}})$ does not depend on q_z, leaving us with six infinite Bragg rods.

The scattering is not infinite in extent in the z direction because of the molecular form factor of the liquid crystal molecules. The molecular form factor is the Fourier transform of molecular charge distribution, crudely approximated by a uniform cylinder of diameter a and length equal to the length of the molecule. When the Fourier transform is done, the maximum of the molecular form factor lies in the plane through the origin of reciprocal space that is perpendicular to the long axis of the molecule.

An important signature of the molecular tilt is the q_z value at which the scattering intensity along a particular Bragg rod is a maximum. This can be calculated by finding the intersection of the Bragg rod with a plane through the origin that is perpendicular to the director

$$\mathbf{n} = (\sin\beta_f\cos\phi, \sin\beta_f\sin\phi, \cos\beta_f). \tag{A8}$$

We use the designation β_f for the tilt of the molecules in the form factor to allow the possibility that the distortion within the plane differs from what is expected from rigid rods. The equation of the plane perpendicular to the director is

$$\mathbf{q}\cdot\mathbf{n} = 0. \tag{A9}$$

The Bragg rods are described by the equation

$$\mathbf{q_{hk}} = h\mathbf{b_1} + k\mathbf{b_2} + q_z\hat{\mathbf{z}}. \tag{A10}$$

Substitute the equation of the Bragg rod for $\mathbf{q}$ and solve for q_z to find the position of the peak along any given rod. The function that gives the peak position as a function of h and k is

$$\begin{aligned}q_z(h,k) = \tan(\beta_f)&\left[\frac{4\pi\cos\beta_p}{\sqrt{3}a^2}\right][(ka_{1y} - ha_{2y})\cos\phi \\ &+ (ha_{2x} - ka_{1x})\sin\phi],\end{aligned} \tag{A11}$$

where a_{1x}, a_{1y}, a_{2x}, and a_{2y} are the components of the direct lattice vectors derived above. We use the above formula for $q_z(h,k)$ and the magnitudes of the in-plane reciprocal lattice vectors $\mathbf{G_{10}}$, $\mathbf{G_{11}}$, and $\mathbf{G_{01}}$ to determine the parameters a, β_p, β_f, and ϕ.

[1] B. I. Halperin and D. R. Nelson, Phys. Rev. Lett. **41**, 121 (1978); D. R. Nelson and B.I. Halperin, Phys. Rev. B **19**, 2457 (1979).

[2] C. W. Garland, J. D. Litster, and K. J. Stine, Mol. Cryst. Liq. Cryst. **170**, 71 (1989).

[3] For a review see P. S. Pershan, *Structure of Liquid Crystal Phases* (World Scientific, Singapore, 1988).

[4] J. J. Benattar, F. Moussa, and M. Lambert, J. Phys. Lett.

(France) **42**, L67 (1981).
[5] P. A. C. Gane, A. J. Leadbetter, and P. G. Wrighton, Mol. Cryst. Liq. Cryst. **66**, 247 (1981).
[6] J. E. Maclennan, U. Sohling, N. A. Clark, and M. Seul, Phys. Rev. E **49**, 3207 (1994).
[7] C. Y. Chao, S. W. Hui, J. E. Maclennan, C. F. Chou, and J. T. Ho, Phys. Rev. Lett. **78**, 2581 (1997).
[8] C. Y. Chao, J. E. Maclennan, P. Z. Pang, S. W. Hui, and J. T. Ho, Phys. Rev. E **57**, 6757 (1998).
[9] G. S. Smith, E. B. Sirota, C. R. Safinya, and N. A. Clark, Phys. Rev. Lett. **60**, 813 (1988).
[10] F. Moussa, J. J. Benattar, and C. Williams, Mol. Cryst. Liq. Cryst. **99**, 145 (1983).
[11] D. Guillon, A. Skoulios, and J. J. Benattar, J. Phys. (France) **47**, 133 (1986).
[12] R. Bartolino, J. Doucet, and G. Durand, Ann. Phys. (N.Y.) **3**, 389 (1978).
[13] P. R. Alapati, D. D. Potukuchi, N. V. S. Rao, V. G. K. M. Pisipati, and D. Saran, Mol. Cryst. Liq. Cryst. **146**, 111 (1987).
[14] D. R. Nelson and B. I. Halperin, Phys. Rev. B **21**, 5312 (1980).
[15] J. V. Selinger and D. R. Nelson, Phys. Rev. Lett. **61**, 416 (1988).
[16] S. B. Dierker and R. Pindak, Phys. Rev. Lett. **56**, 1819 (1986).
[17] S. Krishna Prasad, Geetha G. Nair, and Rajni Kant, Phys. Rev. E **57**, 1789 (1998).
[18] J. Budai, R. Pindak, S. S. Davey, and J. W. Goodby, J. Phys. (France) Lett. **45**, L-1053 (1984).
[19] J. Collett, P. S. Pershan, E. B. Sirota, and L. B. Sorensen, Phys. Rev. Lett. **52**, 356 (1984).
[20] E. B. Sirota, P. S. Pershan, L. B. Sorensen, and J. Collett, Phys. Rev. Lett. **55**, 2039 (1985).
[21] E. B. Sirota, P. S. Pershan, L. B. Sorensen, and J. Collett, Phys. Rev. A **36**, 2890 (1987).
[22] S. Krishna Prasad, D. D. Shankar Rao, S. Chandrasekhar, M. E. Neubert, and J. W. Goodby, Phys. Rev. Lett. **74**, 270 (1995).
[23] A. Aharony, R. J. Birgeneau, J. D. Brock, and J. D. Litster, Phys. Rev. Lett. **57**, 1012 (1986).
[24] D. Y. Noh, J. D. Brock, J. D. Litster, and R. J. Birgeneau, Phys. Rev. B **40**, 4920 (1989).
[25] J. D. Brock, A. Aharony, R. J. Birgeneau, K. W. Evans-Lutterolt, J. D. Litster, P. M. Horn, G. B. Stephenson, and A. R. Tajbakhsh, Phys. Rev. Lett. **57**, 98 (1986).
[26] J. D. Brock, D. Y. Noh, B. R. McClain, J. D. Litster, R. J. Birgeneau, A. Aharony, P. M. Horn, and J. C. Liang, Z. Phys. B: Condens. Matter **74**, 197 (1989).
[27] M. E. Neubert and L. J. Maurer, Mol. Cryst. Liq. Cryst. **43**, 313 (1977). This material was recrystallized twice from ethanol.
[28] J. A. Collett and J. L. Truitt (unpublished).
[29] Interactive Data Language, Research Systems, Inc., Boulder, CO.
[30] R. J. Birgeneau and J. D. Litster, J. Phys. (France) Lett. **39**, 1399 (1978).
[31] We take the *c* lattice parameter from the smectic *G* phase [10] as representing the extended length of the molecule. A slightly smaller value was assumed in Ref. [11].